

STARS

University of Central Florida
STARS

Faculty Bibliography 2010s

Faculty Bibliography

1-1-2012

Adaptive frequency-domain equalization for the transmission of the fundamental mode in a few-mode fiber

Neng Bai
University of Central Florida

Cen Xia
University of Central Florida

Guifang Li
University of Central Florida

Find similar works at: <https://stars.library.ucf.edu/facultybib2010>
University of Central Florida Libraries <http://library.ucf.edu>

This Article is brought to you for free and open access by the Faculty Bibliography at STARS. It has been accepted for inclusion in Faculty Bibliography 2010s by an authorized administrator of STARS. For more information, please contact STARS@ucf.edu.

Recommended Citation

Bai, Neng; Xia, Cen; and Li, Guifang, "Adaptive frequency-domain equalization for the transmission of the fundamental mode in a few-mode fiber" (2012). *Faculty Bibliography 2010s*. 2258.
<https://stars.library.ucf.edu/facultybib2010/2258>



Adaptive frequency-domain equalization for the transmission of the fundamental mode in a few-mode fiber

Neng Bai,* Cen Xia, and Guifang Li

CREOL, The College of Optics & Photonics, University of Central Florida, 4000 Central Florida Blvd., Orlando FL, 32816-2700, USA

*bneng@creol.ucf.edu

Abstract: We propose and experimentally demonstrate single-carrier adaptive frequency-domain equalization (SC-FDE) to mitigate multipath interference (MPI) for the transmission of the fundamental mode in a few-mode fiber. The FDE approach reduces computational complexity significantly compared to the time-domain equalization (TDE) approach while maintaining the same performance. Both FDE and TDE methods are evaluated by simulating long-haul fundamental-mode transmission using a few-mode fiber. For the fundamental mode operation, the required tap length of the equalizer depends on the differential mode group delay (DMGD) of a single span rather than DMGD of the entire link.

©2012 Optical Society of America

OCIS codes: (060.2330) Fiber optics communications; (060.1660) Coherent communications.

References and links

1. F. Yaman, N. Bai, B. Zhu, T. Wang, and G. Li, "Long distance transmission in few-mode fibers," *Opt. Express* **18**(12), 13250–13257 (2010).
2. F. Yaman, N. Bai, Y. K. Huang, M. F. Huang, B. Zhu, T. Wang, and G. Li, "10 x 112Gb/s PDM-QPSK transmission over 5032 km in few-mode fibers," *Opt. Express* **18**(20), 21342–21349 (2010).
3. J. D. Downie, J. E. Hurley, D. V. Kuskonov, C. M. Lynn, A. E. Korolev, and V. N. Nazarov, "Transmission of 112 Gb/s PM-QPSK signals over up to 635 km of multimode optical fiber," *Opt. Express* **19**(26), B363–B369 (2011).
4. R. Ryf, S. Randel, A. H. Gnauck, C. Bolle, A. Sierra, S. Mumtaz, M. Esmaelpour, E. C. Burrows, R. Essiambre, P. J. Winzer, D. W. Peckham, A. H. McCurdy, and R. Lingle, "Mode-Division Multiplexing Over 96 km of Few-Mode Fiber Using Coherent 6 x 6 MIMO Processing," *J. Lightwave Technol.* **30**(4), 521–531 (2012).
5. N. Bai, E. Ip, Y. K. Huang, E. Mateo, F. Yaman, M. J. Li, S. Bickham, S. Ten, J. Liñares, C. Montero, V. Moreno, X. Prieto, V. Tse, K. Man Chung, A. P. Lau, H. Y. Tam, C. Lu, Y. Luo, G. D. Peng, G. Li, and T. Wang, "Mode-division multiplexed transmission with inline few-mode fiber amplifier," *Opt. Express* **20**(3), 2668–2680 (2012).
6. B. Inan, B. Spinnler, F. Ferreira, D. van den Borne, A. Lobato, S. Adhikari, V. A. J. M. Sleiffer, M. Kuschnerov, N. Hanik, and S. L. Jansen, "DSP complexity of mode-division multiplexed receivers," *Opt. Express* **20**(10), 10859–10869 (2012).
7. N. Bai and G. Li, "Adaptive Frequency Domain Equalization for Mode-Division Multiplexed Transmission," in *IEEE Summer Topical Conference*, Seattle, Paper MC4.3 (2012).
8. M. S. Faruk and K. Kikuchi, "Adaptive frequency-domain equalization in digital coherent optical receivers," *Opt. Express* **19**(13), 12789–12798 (2011).
9. S. Haykin, *Adaptive filter theory*, 4th ed. (Prentice-Hall, 2001), Chap. 7.
10. Y. Namihira, Y. Horiuchi, S. Ryu, K. Mochizuki, and H. Wakabayashi, "Dynamic polarization fluctuation characteristics of optical fiber submarine cables under various environmental conditions," *J. Lightwave Technol.* **6**(5), 728–738 (1988).
11. F. Yaman, E. Mateo, and T. Wang, "Impact of Modal Crosstalk and Multi-Path Interference on Few-Mode Fiber Transmission," in *Optical Fiber Communication Conference*, OSA Technical Digest (Optical Society of America, 2012), paper OTu1D.2.
12. C. Koebele, M. Salsi, L. Milord, R. Ryf, C. A. Bolle, P. Sillard, S. Bigo, and G. Charlet, "40km Transmission of Five Mode Division Multiplexed Data Streams at 100Gb/s with low MIMO-DSP Complexity," in *European Conference and Exposition on Optical Communications*, OSA Technical Digest (CD) (Optical Society of America, 2011), paper Th.13.C.3.

1. Introduction

The exponential growth of the internet requires a drastic increase of capacity of optical fiber communication systems. However, the capacity of conventional optical transmission systems based on the single-mode fiber (SMF) has almost reached to the nonlinear Shannon limit. To further increase the capacity, few-mode fiber (FMF) transmission systems have been proposed. With a much larger effective area, nonlinear impairments in FMF transmission systems are reduced in comparison with SMF transmission, enabling higher-capacity for long-haul transmission. Recently, long-haul transmission in the fundamental mode of a FMF has proven to be feasible [1,2]. This approach can be called fundamental mode operation (FMO) of FMF transmission. Due to the multimode nature of the FMF, one of the main impairments of FMO is multi-path interference (MPI) [3]. To reduce MPI, several optical solutions have been proposed and demonstrated. Center launch into the FMF has been shown to be able to selectively excite fundamental mode. Also, the FMF can be designed to support only two mode groups and provide a large enough effective index difference between the two mode groups to suppress inter-mode coupling. However, those constraints on FMF design eventually limit the effective area of FMF.

In the paper, instead of suppressing inter-mode coupling using pure optical techniques, MPI is compensated using digital signal processing (DSP)-based adaptive equalization in the electronic domain at the receiver. This approach enables more flexibility in fiber design to allow a larger number of modes and thus larger effective areas. DSP can also track the temporal variation of the fiber and adaptively optimize its performance to improve system robustness.

Adaptive equalization algorithms have been investigated extensively in the context of single-mode dual-polarization digital coherent optical receiver where linear impairments such as chromatic and polarization mode dispersion (PMD) needs to be compensated. For FMF transmission, inter-mode cross-talk and modal dispersion can be considered as a generalization of polarization coupling and PMD. So far, the investigation of mode cross-talk cancelation algorithm has mainly focused on time-domain equalization (TDE) approaches [4,5]. When the total differential mode group delay of the link is large, the complexity of TDE is unmanageable [6]. We proposed and simulated single carrier adaptive frequency domain equalization (SC-FDE) for mode-division multiplexed (MDM) transmission [7]. It was shown that the computational load for FDE could be significantly lower than TDE. In the paper, the SC-FDE is adapted to fundamental mode operation in FMF. A transmission experiment is also demonstrated showing MPI can be efficiently compensated using SC-FDE.

This paper is organized as follows: Section 2 describes the theory and complexity of SC-FDE for FMO. Section 3 presents performance analysis for both TDE and FDE in a simulated long haul FMF transmission link. In section 4, experimental verification of proposed SC-FDE is provided. Finally, section 5 concludes the paper.

2. Theory

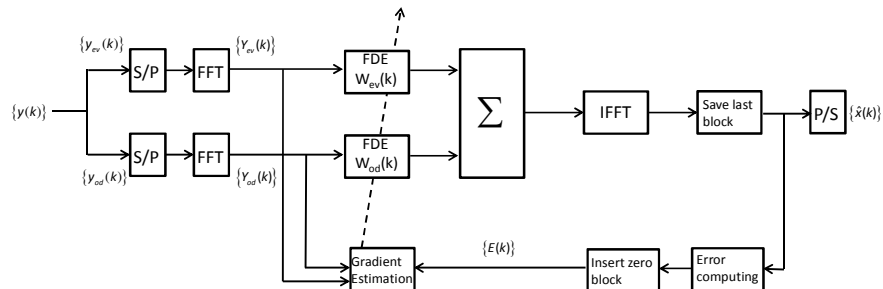


Fig. 1. Block diagram of SC-FDE

Figure 1 shows the schematic of SC-FDE. $\{y(k)\}$ and $\{\hat{x}(k)\}$ represent the input and output signal vectors. To process the input signal at 2 samples per symbol, $\{y(k)\}$ is first divided to the even and odd tributaries as in [8]. After parallelization and fast Fourier transform (FFT), $\{y_{od}(k), y_{ev}(k)\}$ are converted to the frequency domain and multiplied by $\{W_{od}(k), W_{ev}(k)\}$ which are the two inverted channel sub-filters. The overlap-save method is applied to perform linear convolution in the frequency domain. The overlap rate defined by the ratio of block length and filter length is set to be 2 as optimum [9]. By calculating incremental adjustments from gradient estimation, inverted channel sub-filter weights approach the optimum after a stochastic adaptation process. Gradient constraint condition is applied to enforce an accurate calculation of linear convolution. The error signal calculation depends on what type of equalization algorithm is selected. In the paper, the constant modulus algorithm (CMA) is chosen due to its simplicity. The weights of sub-filters are updated at the symbol rate. It should be noted that in a practical environment, the speed of temporal variation of the mode coupling characteristics in the fiber is much lower than the symbol rate. As a reference, for a submarine fiber cable, polarization fluctuation frequency is less than 200Hz [10] while the proposed filters are adapted at tens of GHz. Therefore, temporal variations of mode coupling can be tracked by the adaptive equalizer described here. In contrast to TDE, calculation such as correlation and convolution can be simplified to be multiplication in FDE. Additional computation for conversion between the time and frequency domain can be implemented using FFT algorithm whose complexity is only logarithm with block size. The total complexity (CP) of the algorithm can be measured by the number of complex multiplication per symbol per mode. The CPs for FDE and TDE can be expressed as

$$CP_{FDE} = 6 \log(L_{FDE}) + 10 \quad (1)$$

$$CP_{TDE} = 2L_{TDE} + 2 \quad (2)$$

where L_{FDE} and L_{TDE} are filter lengths of FDE and TDE, respectively.

3. Simulation for long-haul FMF transmission

To evaluate the performance of the proposed FDE method in long-haul FMF transmission systems, long-distance FMF transmission with a span length of 100km was simulated. Without loss of generality, a linear 2 mode propagation model similar to [11] was used. The random distributed mode coupling through FMF is taken into account in the model by multiplying a unitary rotation matrix at the end of every fiber section whose length equals to the coherent length L_c of the FMF ($L_c = 1km$ in our model). Mode scattering factor σ defined in [11] represents the strength of inter-mode coupling. In the simulation, σ was chosen to be $-30dB/km$, which is slightly higher than $-34.4dB/km$ for the FMF used in [12], to demonstrate the capability of MPI cancelation using SC-FDE. The loss and dispersion coefficient for both modes are $0.2dB/km$ and $18ps/nm/km$ respectively [4]. The DMGD is chosen to be $27ps/km$ which equals to that of the FMF used in [4]. The inline amplifier is assumed to compensate loss of the LP_{01} mode while LP_{11} mode receives no modal gain. The noise figure of the amplifier is set to be $5dB$. No fundamental mode filter is applied either in the middle of each span or in front of the amplifier. Mode coupling is assumed to be only contributed by distributed mode coupling. Splicing induced mode coupling or loss is neglected based on previous experimental results [1,2]. A QPSK coherent transmission system with 28 Gbaud/s symbol rate is simulated.

For multi-span FMF transmission, the total DMGD of the link is multiple times of single span. In MDM transmission, the tap length of the equalizer has to exceed the total DMGD

requiring thousands of taps. In the context of FMO transmission, the relation between required length of equalizer and DMGD is first studied. Figure 2(a) plots Q^2 factor as a function of equalizer tap length for a $30 \times 100\text{km}$ transmission at $\text{OSNR} = 17\text{dB}$. The tap number is chosen to be power of 2 for the sake of ease of FFT. The Q^2 factor starts to converge when the tap number increases to 256. This filter length in time (4.6ns) is just slightly larger than single span DMGD (2.7ns) but much smaller than the total DMGD of the link (81 ns). The result suggests that for FMO transmission, the minimum required filter length equals to single span DMGD but not the total DMGD of the link. It is straightforward to understand this phenomenon from the nature of MPI. For simplicity, the mode coupling process is assumed to be modeled as collection of discrete random coupling events with separation distance equal to the coherent length of the fiber. For a two mode fiber, the path of a MPI signal is of the form “ $\text{LP}_{01} \rightarrow \text{LP}_{11} \rightarrow \dots \rightarrow \text{LP}_{01}$,” with an even number of coupling events. Since mode scattering factor normally is very small, the MPIs induced by more than 2 coupling events are negligible. If only the “ $\text{LP}_{01} \rightarrow \text{LP}_{11} \rightarrow \text{LP}_{01}$ ” case is considered, the relative delay between MPI components and the main signal which stays in LP_{01} depends on the distance between 2 coupling locations. During the section between couplings, MPI component propagates in LP_{11} mode. If the coupling distance is larger than the span length, interference signal goes through an amplifier in the LP_{11} mode, which has zero modal gain. Therefore, only MPI components with a pair of couplings inside a single span could survive at the end of the link. Indeed, the assumption is verified also as shown in Fig. 2(b), which plots filter weights of a sub-filter for the odd samples. Magnitude less than -30dB is observed for those taps with index larger than 0. It indicates that intensity of MPI with group delay larger than DMGD of a single span is infinitesimal.

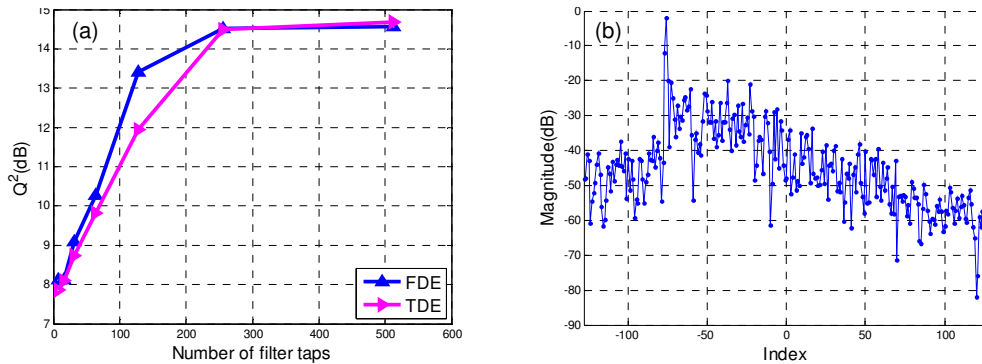


Fig. 2. (a) Q^2 factor Vs. the number of total filter taps (b) Magnitude of sub-filter tap weights for $30 \times 100\text{km}$ FMF transmission link at OSNR of 17dB.

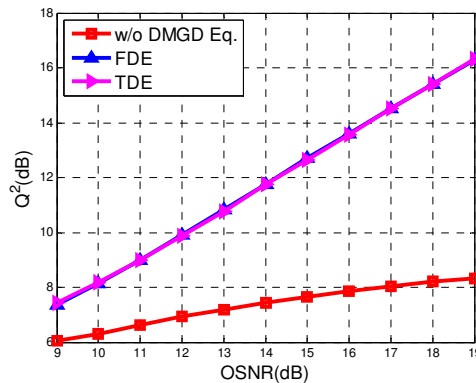


Fig. 3. Q^2 factor Vs. OSNR.

Long-haul transmission simulation results are shown in Fig. 3 and Fig. 4. Simulations for $30 \times 100\text{km}$ transmission at different OSNR levels were performed. Figure 3 illustrates the result curve. The performance improvement due to adaptive DMGD/MPI equalization grows as OSNR increases, as shown in Fig. 3. Figure 4 demonstrates Q^2 factor as a function of distance ranging from 100km to 5000km. Noise loading at the receiver was used to fix the OSNR at 17dB. Without DMGD equalization, system performance degrades rapidly as the transmission distance increases due to accumulated MPIs. With equalization, the performance increases as much as 7 dB in terms of Q^2 factor. For all distance, both TDE and FDE have total 256 taps. At the same performance, FDE saves 88.7% computational load compared to TDE.

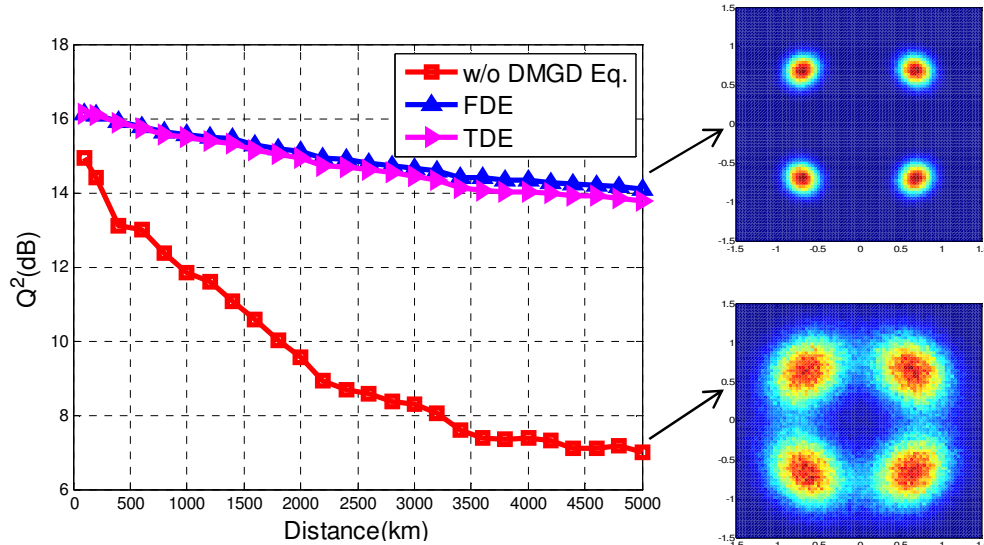


Fig. 4. Q^2 factor Vs. distance and the constellation diagrams for two Q^2 values are also shown on the right hand side.

4. Experiment

To experimentally demonstrate SC-FDE, we use a 1 km step-index few-mode fiber with a core diameter of $13.1\mu\text{m}$. The FMF effectively guides 2 spatial mode groups, LP_{01} and LP_{11} at 1550nm. The effective area of the fiber is $113\mu\text{m}^2$. Although only single span transmission is performed, according to section 3, for FDE or TDE, multi-span transmission can be compensated using equalizer with the same filter length as that for a single span.

4.1 Impulse response and DMGD

The fiber is first characterized by measuring the impulse response which is shown in Fig. 5. A pulse train at a repetition period of 8ns is generated by modulating the amplitude of the continuous wave (CW) light from an external cavity laser (ECL). The pulse width is 200ps. The pulsed light is then butt coupled from a single mode fiber (SMF) into the FMF. After 1km transmission, the output light is coupled back into a SMF which is connected with a sampling oscilloscope. When the position of SMF at the excitation stage is aligned with the center of the FMF, only one pulse is found in the period. It confirms again that mode coupling at interconnection between SMF and FMF can be suppressed to a negligible level under center launching condition. Due to short distance, the temporal spread of the pulse from chromatic dispersion (CD) is fairly small. When the SMF was offset by a few microns from the center, a weak replicate pulse starts to grow due to the excitation of the LP_{11} mode. It should be noted that modal effective index difference between LP_{01} and LP_{11} is about 2×10^{-3}

which is large enough to suppress mode coupling. The low mode coupling can be verified in the impulse response where the power level between two distinct pulses is very low. The weak hump between two pulses is caused by imperfect frequency response of the modulator driver. In addition, the DMGD can be estimated by measuring the temporal separation between the two pulses. At 1550nm, the DMGD is about 3780ps for 1km fiber which is approximately equal to a 140km span of FMF used in the mode-division multiplexing experiment of [4].

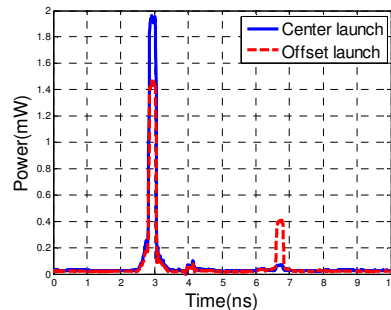


Fig. 5. Impulse response of a FMF at 1550nm.

4.2 Transmission experiment

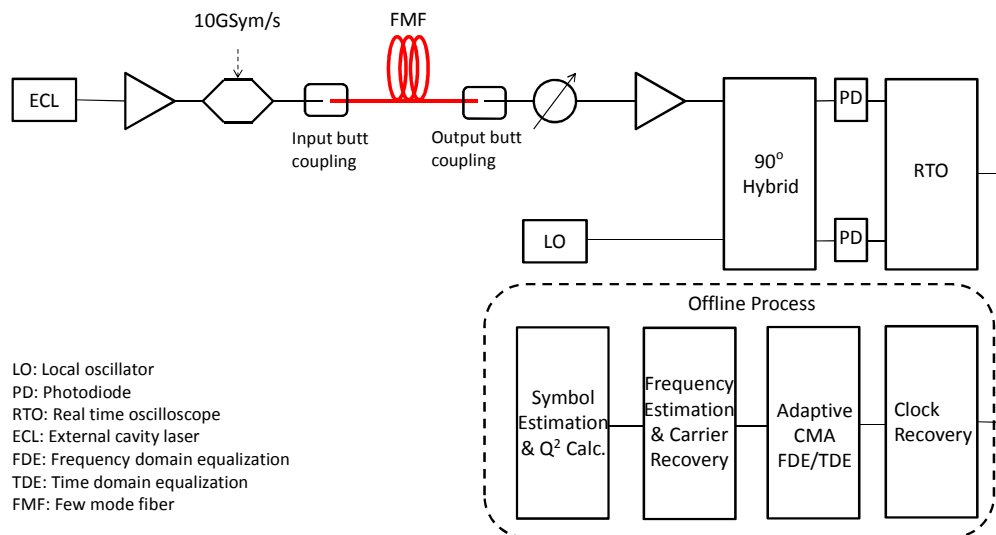


Fig. 6. Transmission experiment setup

The transmission experimental setup is illustrated in Fig. 6. A 10 Gbaud/s BPSK signal was generated by using an amplitude modulator and a pattern generator. Both ends of the FMF were butt-coupled with SMFs, in the same way as in the impulse response measurement. A high precision variable attenuator and a post-amplifier were used to adjust the optical signal-to-noise ratio (OSNR) at the coherent receiver. The signal was then sent to a 90 degree hybrid followed by two photo-detectors measuring the real and imaginary parts of the complex signal. Finally, the electric waveforms were fed into a real-time oscilloscope with a 40GHz sampling rate. 5×10^5 samples were then recorded and processed offline.

As we observed in section 4.1, due to the relatively short transmission distance and low inter-mode coupling, distributed mode coupling are negligible in the fiber. To emulate multipath interference, the SMF was intentionally offset several microns to excite both LP_{01}

and LP_{11} modes. The offset launch condition is equivalent to a discrete mode coupling at the beginning of the FMF. At the output end of FMF, the FMF-SMF butt coupling was also misaligned to receive powers from both the LP_{01} and LP_{11} modes. In offline DSP, both adaptive TDE and FDE were applied after clock recovery to compare the performance as well as efficiency of these two approaches. In order to compensate DMGD, the equalizers with a total tap length of 128 were used for both TDE and FDE. Due to the fact that the symbol rate for experiment is lower than that in the simulation, the total tap length is half that in the simulation. Figure 7 shows Q^2 factor as a function of OSNR at the receiver. For back-to-back measurements, center launch and offset launch without DMGD equalization, only a 16 taps adaptive finite impulse response (FIR) filter was applied to equalize the CD or other impairments such as the frequency response of modulator driver and real time oscilloscope (RTO). Due to MPI, offset launch suffered high penalty compared to center launch case. At low OSNR, the performance of offset launching with equalization is approximately equal to center launching which verifies that both TDE and FDE effectively reduced the impact of MPI. Moreover, according to Eqs. (1) and (2), the computational complexity of FDE is only 20% of TDE.

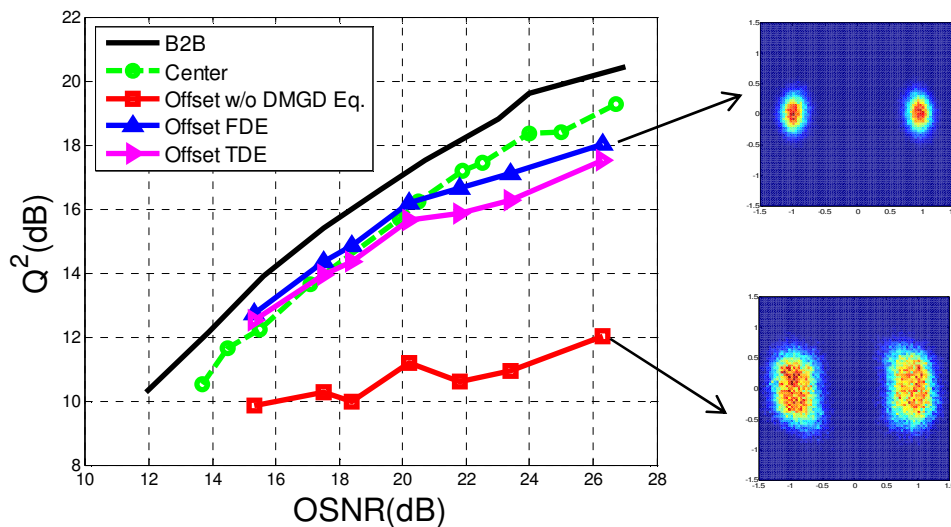


Fig. 7. Q^2 Vs OSNR and the constellation diagrams for two Q^2 values are also shown on the right hand side

In Fig. 8, the complex values of a frequency domain sub-filter tap weights are plotted in the time domain. It can be observed that two distinct peaks which agree well with the impulse response measured in Fig. 5 under offset launching condition. The left main peak corresponds to the signal launched into LP_{01} mode while the right weak peak relates to signal coupled to LP_{11} mode at the beginning of the fiber. Two signal components propagate at different group velocities. The temporal separation between two dominant peaks (~ 3800 ps) is very close to the DMGD we previously measured.

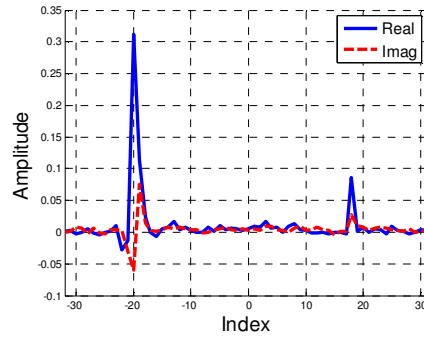


Fig. 8. Typical sub-filter (odd) tap weights for FDE.

5. Conclusion

An SC-FDE algorithm for mitigating MPI in the fundamental-mode transmission in a FMF is proposed and experimentally demonstrated. It is shown that SC-FDE significantly reduces the computational complexity compared to TDE while maintaining similar equalizing performances. The FDE algorithm potentially enables enhanced the transmission capacity using ultra large effective area FMF with MPI.